Environmental Advances 6 (2021) 100122

Contents lists available at ScienceDirect

Environmental Advances

journal homepage: www.sciencedirect.com/journal/environmental-advances

Differential impacts of COVID-19 lockdowns on $PM_{2.5}$ across the United States

Kevin L. Chen [a], Lucas R.F. Henneman [b], Rachel C. Nethery [*,a]

[a] Department of Biostatistics, Harvard T.H. Chan School of Public Health, 655 Huntington Ave, Boston, MA, USA
[b] Department of Civil, Environmental, and Infrastructure Engineering, George Mason University, 4400 University Dr, Fairfax, VA, USA

ARTICLE INFO

Keywords:
COVID-19
Air pollution
Air quality
Stay-at-home
Environmental policy
Causal inference

ABSTRACT

The COVID-19 pandemic has induced large-scale behavioral changes, presenting a unique opportunity to study how air pollution is affected by societal shifts. At 455 $PM_{2.5}$ monitoring sites across the United States, we conduct a causal inference analysis to determine the impacts of COVID-19 lockdowns on $PM_{2.5}$. Our approach allows for rigorous confounding adjustment with highly spatio-temporally resolved effect estimates. We find that, with the exception of the Southwest, most of the US experienced increases in $PM_{2.5}$ compared to concentrations expected under business-as-usual. To investigate possible drivers of this phenomenon, we use a regression model to characterize the relationship of various factors with the observed impacts. Our findings have immense environmental policy relevance, suggesting that mobility reductions alone may be insufficient to substantially and uniformly reduce $PM_{2.5}$.

1. Introduction

Acute widespread social, behavioral, and economic changes have occurred across the United States (US) in the wake of the COVID-19 pandemic. Most notably, mobility levels decreased substantially (Badr et al., 2020; Jacobsen and Jacobsen, 2020; Lasry et al., 2020) nationwide during the initial "lockdown period" in March and April 2020 as a result of changes in human behavior and other nonpharmaceutical interventions, such as government-imposed stay-at-home orders, in response to the rapid spread of the virus. The unprecedented actions taken to curb the spread of COVID-19 have created a unique "quasi-experiment" that can be leveraged to study the effect of large-scale behavioral change on air quality.

Exposure to fine particle matter, $PM_{2.5}$, has been shown to have significant adverse health effects, including respiratory and cardiovascular morbidity and mortality (Dominici et al., 2006; Pope, 2000; Xing et al., 2016). To create effective policy to limit $PM_{2.5}$ exposure, it is crucial to understand the impact of reductions in certain emission-generating human behaviors on ambient concentrations. Studies of other, smaller scale quasi-experiments have provided some of the strongest evidence for the health impacts of air pollution and effective reduction strategies, e.g., the ban of bituminous coal in Dublin (Clancy et al., 2002), restrictions on transportation and industrial activities during the 1996 Atlanta (Friedman, 2001) and 2008 Beijing Olympic Games (Hou et al., 2010; Li et al., 2010).

A review of literature on the impacts of COVID-19 lockdowns on urban air pollution by Gkatzelis et al. (2021) identifies more than 200 published papers on the topic; however, the overwhelming majority of these studies were not conducted in the US. Among those that are US-focused, most have studied lockdown effects on air quality using data from a single or a few monitors (Chen et al., 2020) or using nationwide and/or statewide averages of monitored values (Shakoor et al., 2020). However, due to the vast differences across space in source-specific contributions to $PM_{2.5}$, the crudeness of these aggregated analyses limits their policy relevance. Several studies also utilize chemical transport models in their analyses (Barré et al., 2021; Menut et al., 2020; Putaud et al., 2021), though these approaches make a number of assumptions that may not hold in practice. In our study, we estimate the effects of the lockdown on observed $PM_{2.5}$ concentrations at each of 455 individual monitors in the Environmental Protection Agency (EPA) monitoring network located throughout the contiguous US. The high spatial resolution of our effect estimates, along with their basis in empirical data, provides more specific policy insights and enables deeper investigation into the factors influencing lockdown-related changes in $PM_{2.5}$.

While a monitor-level analysis of lockdown effects in the US has been

* Corresponding author.
E-mail addresses: kevinleechen@g.harvard.edu (K.L. Chen), lhennem@gmu.edu (L.R.F. Henneman), rnethery@hsph.harvard.edu (R.C. Nethery).

https://doi.org/10.1016/j.envadv.2021.100122
Received 19 July 2021; Received in revised form 23 September 2021; Accepted 1 October 2021
Available online 7 October 2021

published (Archer et al., 2020), our study aims to produce more robust effect estimates by employing causal inference methods. Even in the context of quasi-experimental conditions, isolating the effects of COVID-19 interventions on air pollution in general cannot be achieved through simple before-and-after comparisons, nor comparison to concentrations in the previous year(s), strategies that are used in much of the existing literature and oft-cited in news media. Numerous time-varying factors that influence air pollution levels, both observable and unobservable, are unaccounted for with such approaches, e.g., meteorology, year-to-year trends, and seasonality. For example, $PM_{2.5}$ levels have decreased 44% in the US since 2000 (U.S. Environmental Protection Agency, 2020c). In their review, Gkatzelis et al. (2021) note that much of the available literature on lockdowns and air quality does not account for year-to-year variability and other time-varying factors that have a significant effect on air pollution. In the only existing monitor-level analysis in the US, Archer et al. (2020) compare observed $PM_{2.5}$ concentrations to 5-year monthly average reference concentrations. As a result, more rigorous approaches are needed to account for pollution trends and time-varying confounders as a means of truly characterizing the causal effects of pandemic-related behavioral changes.

The aims of our study are best represented as a two-stage approach: first, we estimate the lockdown-attributable daily changes in $PM_{2.5}$ concentrations at 455 monitoring sites using a causal inference approach that can adjust for both observed and unobserved time-varying contributors to $PM_{2.5}$. Formally, at each monitor, we estimate the $PM_{2.5}$ concentrations that would have been expected each day in the absence of the COVID-19 pandemic and subsequent interventions (the “counterfactual”) and compare these to the corresponding observed levels at the monitor during the lockdown. Second, we use these effect estimates to identify environmental, geographical, mobility, and socio-economic factors that are associated with changes in $PM_{2.5}$ during the lockdown. We also quantify the impact of these short-term $PM_{2.5}$ changes on respiratory and cardiovascular disease hospitalizations using the EPA’s Core Particulate Matter Health Impact Functions.

2. Materials and methods

All data preparation and analyses are conducted in `R` statistical software version 4.0.2.

For consistency, we define the “lockdown period” for each ground monitor site as beginning on the declared state of emergency for the corresponding contiguous US state (or District of Columbia) and ending on the earlier of either April 30, 2020 or on the day businesses began to reopen in that state (Raifman et al., 2020). The state-level lockdown period dates used throughout this study are given in Appendix Table A.1. Daily average $PM_{2.5}$ concentrations between 2010 and 2019 from 1,580 monitor sites in the continental US are obtained from the EPA Air Quality System (AQS) (U.S. Environmental Protection Agency, 2020a). For 2020, daily average $PM_{2.5}$ concentrations are obtained from the EPA AirNow system (U.S. Environmental Protection Agency, 2020a), where monitor data are made available prior to their integration into AQS, which occurs approximately twice per year. Daily meteorological factors (total precipitation, maximum temperature, maximum relative humidity, wind speed, and wind direction), day of the week, and season are obtained from Google Earth Engine (Gorelick et al., 2017), aggregated to the county level (for meteorology), and merged by county and day with the monitor-level $PM_{2.5}$ data. Because some monitors have prohibitive amounts of missing $PM_{2.5}$ measurements, we set inclusion criteria to select the monitors with sufficient data to establish the time trends needed for our analyses. Starting with 1,580 monitor sites with $PM_{2.5}$ measurements between 2010–2020, we remove monitors (1) with no $PM_{2.5}$ measurements during the defined lockdown period for their respective state, roughly mid-March to late-April of 2020 (918 monitors); (2) with less than 30 days of data during the lockdown period (23 monitors); (3) with no data prior to 2016 (117 monitors); or (4) with data entirely missing for five or more total years 2010–2019 (67 monitors). After applying these exclusion criteria, 455 monitors remain to be used in our analyses.

In our analysis, we rely solely on observed $PM_{2.5}$ concentrations from ground monitors. Our goal is to estimate the daily $PM_{2.5}$ concentrations that would have been expected at each monitoring site during the lockdown period under a business-as-usual scenario (i.e., without the lockdowns or the non-mandated personal behavioral changes that took place due to COVID-19 during the same period). Hereafter we refer to these as the “counterfactual $PM_{2.5}$ concentrations”. As a result of long-term, seasonal and daily trends in $PM_{2.5}$, complex meteorological variability, and other potential unobserved confounding factors, $PM_{2.5}$ concentrations from a single previous year cannot be directly utilized to infer the counterfactual $PM_{2.5}$ concentrations, nor can a simple average of $PM_{2.5}$ concentrations over multiple years of historical data. We therefore use a causal inference approach often referred to as the “synthetic control method” (SCM) to estimate counterfactual $PM_{2.5}$ concentrations (Abadie et al., 2010; Athey et al., 2020; Xu, 2017).

SCM was created to analyze the effects of a policy or intervention on an outcome in the context of case studies. It leverages time series containing pre- and post-intervention outcome data from (1) a single unit that received an intervention (the “treated” unit) and (2) a set of control units that did not receive the intervention. Conceptually, using the pre-intervention data from both treated and control units, it creates a weighted average of the time series from the control units that best captures the pre-intervention trends in the time series for the treated unit. Then that same weighted average of the control units’ outcomes is used to estimate the outcome that would have been expected in the treated unit during the post-treatment period, in the absence of the intervention (the counterfactual outcome). This weighted average created by SCM is called a “synthetic control”. Formally, the optimal weights are identified by obtaining a latent factor representation of the multivariate time series data. SCM is flexible enough to account for both time-varying and time-invariant confounders of the intervention effect under mild assumptions. In addition, it accounts for any remaining pre-treatment missing data by imputation. Xu (2017) conducted a number of simulations demonstrating the superior performance of SCM over other commonly used estimators in quasi-experimental settings, such as the difference-in-differences estimator that is used in a number of studies of lockdown effects on air pollution (He et al., 2020; Liu et al., 2021).

Adapting the SCM framework to our application, for a given monitor, we consider each year 2010–2020 to be a “unit”, and the time series of $PM_{2.5}$ concentrations for each year (limited to months January-April) are the outcomes. 2020 is considered the treated unit and all other years are controls. Thus, SCM will create a weighted average of daily 2010–2019 $PM_{2.5}$ concentrations at that monitor, and use that weighted average to estimate the counterfactual daily $PM_{2.5}$ concentrations during the lockdown period. The weights are selected to result in a synthetic 2020 time series that provides the closest approximation of the 2020 pre-lockdown observed time series of $PM_{2.5}$ concentrations.

To create a proper synthetic control, we must ensure that the time series from each year are aligned so that the day represented at a given position in the time series is comparable across years. Because $PM_{2.5}$ exhibits weekday and weekend trends that must be accounted for when creating the synthetic control, we align the time series based on day-of-week rather than day-of-year. In particular, we let the time series for each year start on the first Monday of the year, so that aligning entries in the time series represent the same day-of-week and only a few days difference in day-of-year. The values of the synthetic times series during the lockdown represent our best guess at what $PM_{2.5}$ concentrations would have been under a “business-as-usual” scenario, simultaneously accounting for daily, seasonal, and long-term $PM_{2.5}$ trends.

We implement SCM separately on the data from each of the 455 monitors using the *gsynth* package in R (Xu, 2017) with a matrix completion estimator (Athey et al., 2020). In addition to the default latent factor representation used by SCM, we include in the model fixed effects for year and time series position and adjust for both weather (maximum temperature, maximum relative humidity, precipitation, wind speed, and wind direction) and seasonality (month of year) as time-varying covariates. At each monitor, we take the simple difference of the observed $PM_{2.5}$ concentrations during the lockdown and the SCM-estimated counterfactual $PM_{2.5}$ concentrations to obtain the lockdown-attributable changes in $PM_{2.5}$ for each day. Cumulative estimates of lockdown-attributable changes in $PM_{2.5}$ reported hereafter are averages of these daily effect estimates across all days in the lockdown period for the specified monitor. For consistency with the causal inference literature, we refer to these estimates as "average treatment effects on the treated" (ATTs).

Diagnostic plots are manually inspected for each monitor to assess SCM model fit. In addition, we conduct a formal evaluation of the accuracy of the SCM method relative to another commonly used approach for lockdown air quality effect estimation (Gkatzelis et al., 2021). First, we refit our SCM models for each monitor, removing all 2020 data and designating 2019 as a fabricated treated unit, and use SCM to predict $PM_{2.5}$ concentrations in the 2019 post-treatment period (mid-March through the end of April to seasonally align with the 2020 lockdown period). As no major nationwide behavioral shifts occurred at this time in 2019, small differences between predicted and observed $PM_{2.5}$ concentrations indicate strong model performance. For comparison, for each monitor, we also created predictions of $PM_{2.5}$ for the fabricated treated unit by taking a simple average of concentrations during the same period over the preceding 3 years (2016–2018), which is a commonly-used approach for performing these types of analyses. We compare both sets of predictions with the empirical $PM_{2.5}$ concentrations observed in 2019, and we compute the root mean square error (RMSE) at each monitor.

In the second stage of modeling, we use a linear regression model to identify features associated with the estimated lockdown-attributable changes in $PM_{2.5}$. The effect of meteorological variables adjusted for in the first stage of modeling is first subtracted from the treatment effect estimates, to remove any influence of unusual meteorology on changes in $PM_{2.5}$ during lockdown. Each monitor is then linked to a large set of features of the county it resides in. The units of analysis in this model are monitors, and the outcome in the regression model is the monitor-level estimated lockdown-attributable change in $PM_{2.5}$. Features included as predictors in the model are: residential emissions, industrial processes emissions, industrial boiler emissions, dust emissions, agriculture emissions, mobile emissions, mobility change relative to baseline, socioeconomic and demographic variables (proportion of population age 65+, racial composition, poverty rate, population density), urbanization level (classified into large central metro, large fringe metro, medium metro, and other), and US census-defined regions (Midwest, Northwest, South, and West). All features are obtained at the county-level and each monitor is assigned the features of the county in which it lies. Descriptions of each variable and data sources are provided in Appendix Table A.2.

Mobility change was measured relative to a February 2020 baseline and defined by quantifying the number of Bing tiles Facebook users are seen in during a day (Herdağdelen et al., 2020). Socioeconomic and demographic variables were taken from the 2018 5-year American Community Survey (U.S. Census Bureau, 2019). Data on sources of emissions were obtained from the EPA 2017 National Emissions Inventory reports (U.S. Environmental Protection Agency, 2014; 2017). Urban-rural classifications are obtained from 2013 National Center for Health Statistics Urban-Rural Classification Scheme for Counties (Ingram and Franco, 2012) and large central metro is used as the reference variable in the model. Areas classified as smaller than "medium metro" are grouped into a variable called "other". The Midwest Region is the reference variable in the model for region indicators. Coefficient estimates and 95% confidence intervals are reported.

We use exposure-response functions from the EPA's Core Health Impact Functions for Particulate Matter and Hospital Admissions (U.S. Environmental Protection Agency, 2020b) to characterize associations between short-term $PM_{2.5}$ exposure and (1) respiratory disease hospitalization risk and (2) cardiovascular disease hospitalization risk (Bell, 2012; Kloog et al., 2012). To estimate the health impacts of lockdown-attributable $PM_{2.5}$ changes across the entire continental US, we first interpolate the estimated monitor-level $PM_{2.5}$ changes to obtain an estimate for each county (including those without an included monitor). Inverse distance weighting is used to interpolate the estimated effects at the monitor sites to each county's centroid, and the resulting interpolated values are treated as each county's lockdown-attributable change in $PM_{2.5}$. We insert each county's $PM_{2.5}$ changes into the pre-existing short-term exposure-response functions for each hospitalization type for individuals 65+ (a log-linear model with parameter estimates taken from Kloog et al. (2012) and Bell (2012)) to obtain an estimate of its change in hospitalization incidence rate. Baseline incidence rates are calculated using a weighted average of hospitalization incidence rates for people age 65+ (3.352 respiratory hospitalizations/100 people per year; 5.385 cardiovascular hospitalizations/100 people per year). The change in incidence rate is then used to obtain the county's absolute change in hospitalizations for each of the two health outcomes in people age 65+. These values are summed across each US census region and scaled to account for the number of days in the state's lockdown period, i.e., the number of days of the specified change in $PM_{2.5}$ exposure. We also estimate the changes in hospitalization incidence that would have occurred if these $PM_{2.5}$ changes had been sustained for an entire year.

3. Results and discussion

For each ground monitor, we use SCM to estimate the "counterfactual $PM_{2.5}$ concentrations" during the corresponding defined lockdown period, i.e., the daily concentrations that would have been expected during the 2020 lockdown period in the absence of the lockdown or any non-mandated personal behavioral changes that took place due to COVID-19 during same period. The counterfactual concentrations are then used to obtain the estimated lockdown-attributable changes in $PM_{2.5}$ concentrations (ATTs) at each monitor. Fig. 1 maps the ATTs at each monitoring site as well as showing a smoothed map of these estimates, interpolated using inverse distance weighting. Negative ATT values, depicted in green, indicate that the location experienced a lockdown-attributable decrease in $PM_{2.5}$ concentrations, while positive (orange/red) values represent lockdown-attributable increases.

We find that, during the COVID-19 lockdowns, $PM_{2.5}$ increased across most of the US compared to what would have been expected under a business-as-usual scenario. We henceforth refer to smaller lockdown-attributable increases or larger lockdown-attributable decreases as "smaller increases", and larger lockdown-attributable increases or smaller lockdown-attributable decreases as "larger increases". The maps suggest that any lockdown-attributable decreases in $PM_{2.5}$ are generally limited to areas of the Western and Southwestern United States. However, substantial lockdown-attributable increases were observed in much of the South, Midwest, and Pacific Northwest. Stratifying by US Census-defined regions, we find average region-wide increases of 1.19 $\mu g/m^3$, 1.11 $\mu g/m^3$, 1.94 $\mu g/m^3$, and 0.80 $\mu g/m^3$ for the Northeast, South, Midwest, and West, respectively. Over the entire country, we observe an average increase of 1.36 $\mu g/m^3$ attributable to pandemic interventions.

Monitor-level model fit plots indicate that the synthetic controls created by SCM are effectively capturing 2020 pre-lockdown $PM_{2.5}$ trends (Appendix Figure A.3). The results of our assessment of SCM predictive accuracy for 2019 are displayed in Appendix Figure A.1. The blue histogram shows the distribution of the monitor-level RMSEs for SCM predictions (gsynth) and the red histogram shows the monitor-level RMSEs for the historic 3-year averaging method. The lower RMSEs for SCM indicate improved predictive performance and better ability to

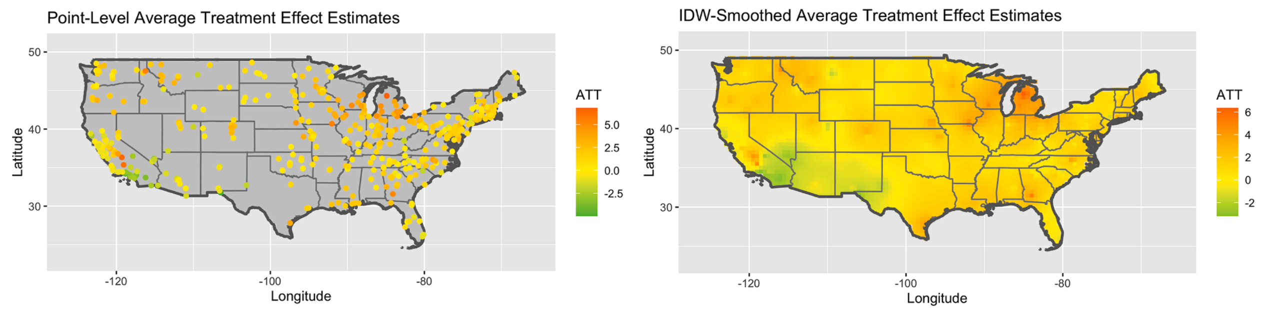

Fig. 1. (Left) Monitor-level estimated average treatment effect on the treated ("ATT"), in μg/m^3; i.e., the average $PM_{2.5}$ change attributable to COVID-19 interventions over the lockdown period. (Right) ATTs (in μg/m^3) smoothed across the US using inverse distance weighting.

capture trends in $PM_{2.5}$ relative to simple historic averaging.

The formation of $PM_{2.5}$ is known to be a very complex process– along with being directly emitted, much of it is formed secondarily in the atmosphere from other pollutants. To better understand factors that may have contributed to the heterogeneity in lockdown-attributable $PM_{2.5}$ changes detected by our study (Fig. 1), we investigate associations between the monitor-level effect estimates and the environmental, geographical, regional, meteorological, mobility, and socioeconomic conditions in the area surrounding the monitor. Using the estimated lockdown-attributable $PM_{2.5}$ changes as the outcome, we fit a linear regression model. Using this model, we find that historic industrial boiler emissions and county population density have significant positive associations with lockdown-attributable increases in $PM_{2.5}$, while a significant negative association was observed for relative mobility decrease, proportion of population age 65+, and the West region (relative to the reference region Midwest). In addition, relative to the most urban counties (reference group), all less urban county classifications show significant positive associations with lockdown-attributable increases in $PM_{2.5}$. A summary of model estimates is provided in Fig. 2.

Although areas with larger decreases in mobility tended to experience smaller increases in $PM_{2.5}$, our results suggest that any positive air quality impacts of these large-scale mobility decreases were, on average, insufficient to offset other non-meteorological factors promoting $PM_{2.5}$ formation. Supporting this finding is Table 1, which shows the amount

Table 1
Sources of $PM_{2.5}$ emissions by US Census region, in tons, with corresponding proportion of total regional $PM_{2.5}$ emissions in parentheses from the EPA 2014 National Emissions Inventory (U.S. Environmental Protection Agency, 2014).

Type	Northeast	South	Midwest	West	US Total
Stationary	260,853 (82.7%)	1,181,440 (60.9%)	1,262,981 (81.1%)	568,122 (42.4%)	3,273,396 (63.5%)
Mobile	41,432 (13.1%)	129,699 (6.9%)	97,710 (6.3%)	64,945 (4.9%)	333,786 (6.5%)
Other	13,091 (4.2%)	629,734 (32.4%)	196,898 (12.6%)	705,595 (52.7%)	1,545,318 (30.0%)

of $PM_{2.5}$ emissions for each US Census region stratified by source (U.S. Environmental Protection Agency, 2014). Regions with historically higher emissions from stationary sources (i.e. fuel combustion sources such as power plants, solvents, agriculture, and other industrial processes) correspond to areas in which we found higher propensity for lockdown-attributable increases in $PM_{2.5}$ during the lockdown. Additionally, mobile sources have a comparatively much smaller impact on $PM_{2.5}$ emissions (Table 1).

We also investigate these lockdown-attributable $PM_{2.5}$ changes relative to a "baseline" $PM_{2.5}$ level prior to the pandemic. For each monitor site, we calculate the baseline as the average $PM_{2.5}$

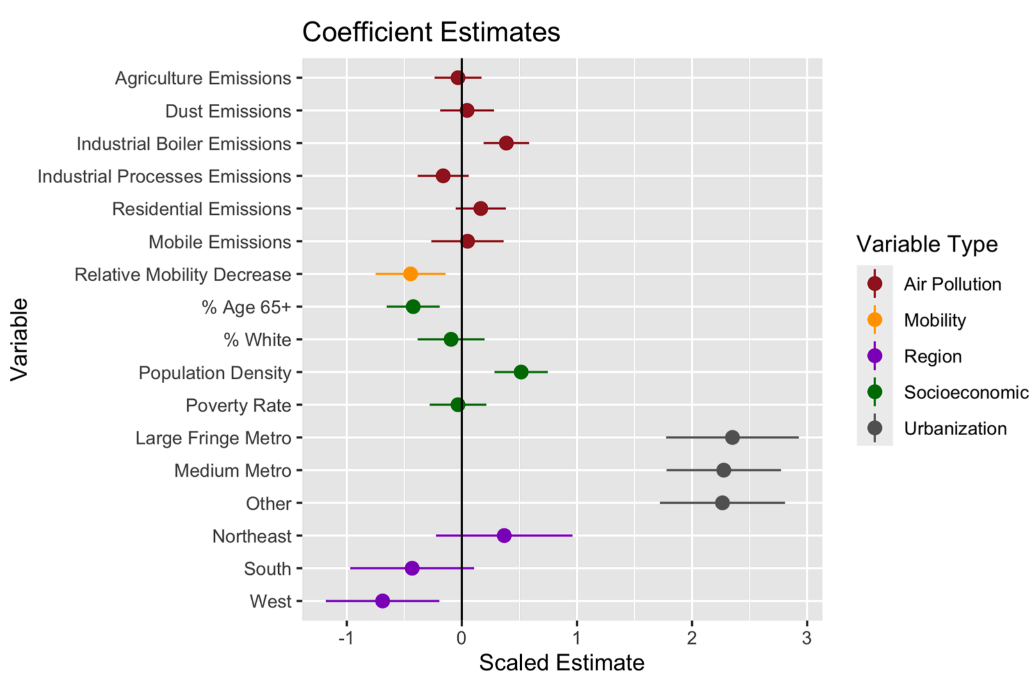

Fig. 2. Coefficient estimates and 95% confidence intervals from linear regression model.

concentration observed in the month of April for 2017–2019. In a linear model, we find a nonsignificant, negative association (-0.076, 95% CI [-0.165, 0.014]) between baseline $PM_{2.5}$ and the estimated lockdown-attributable changes in $PM_{2.5}$.

Additionally, we assess the sensitivity of our findings to a 1–2 day spike in $PM_{2.5}$ of unknown origin that we observed during the lockdown period for many monitors in the Midwest. To do so, we identify and remove these outlier days, defined as days on which $PM_{2.5}$ levels spiked to 35 $\mu g/m^3$ or higher, from our ATT estimates for all monitors. However, the removal of these outliers did not significantly affect the results (see Appendix Figure A.2).

We calculate the expected impacts of the estimated lockdown-attributable changes in $PM_{2.5}$ on respiratory and cardiovascular disease hospitalizations in the age 65+ population for each county in the US, using the EPA's Core Health Impact Functions for Particulate Matter (U.S. Environmental Protection Agency, 2020b). We sum these changes across counties within each US region to obtain the results displayed in Table 2. The values in Table 2 are thus estimates of the net change in hospitalizations over the given US Census region which would be expected due to our previously estimated lockdown-attributable $PM_{2.5}$ changes. For example, we estimate that there was a net increase of 83 respiratory disease hospitalizations over the entire Midwest region during the lockdown period, and a net decease of 14 respiratory disease hospitalizations over the West region during the same time period. As a reference, estimated baseline hospitalizations are given in Appendix Table A.3. However, we acknowledge that the usage of these dose-response functions cannot not fully characterize the complexity involved in estimating the health effects of $PM_{2.5}$ and that such usage requires a number of simplifying assumptions. Although they are not estimated from empirical health data and involve strong assumptions, health impact estimates from dose-response functions are commonly considered in the environmental policy/cost-benefit analysis context, which motivates their inclusion here. These estimates are small relative to the overall $PM_{2.5}$ burden in the US (Murray et al., 2020), as expected given the short time-scale and the varying directions of the $PM_{2.5}$ changes.

There are a number of limitations of our study. First, due to sporadic data collection at certain monitor sites, there is a considerable amount of missing $PM_{2.5}$ data, particularly in prior years that are used to establish expected $PM_{2.5}$ in the absence of the lockdown. However, much of the missingness is by-design due to EPA monitoring procedures, and we have set fairly stringent monitor inclusion criteria for our analyses to ensure that observed data are sufficient to capture important trends. In addition, our models are flexible enough to account for some missing data and we have visually inspected our results to ensure suitable model fit pre-lockdown (Appendix Figure A.3) as well as conducted a formal evaluation demonstrating the predictive accuracy of our model as described in the Methods (Appendix Figure A.1). Furthermore, the heterogeneity of lockdown procedures, stringency, and adherence to advisories creates difficulty in a clear definition of the lockdown period. However, the time period we have defined was the period of the most acute lockdowns and we have further mitigated this issue by using consistent criteria for each state.

Additionally, we note that total $PM_{2.5}$ is only one aspect of air pollution that is relevant to human health. While we report lockdown-attributable increases in total $PM_{2.5}$ concentrations in many areas of the US, lockdown-attributable decreases in other pollutants such as NO_2 and in certain $PM_{2.5}$ components, as found in other studies (Berman and Ebisu, 2020; Chen et al., 2020), demonstrate that reductions in mobile-source emissions were effective in decreasing certain other hazardous pollutants. The scope of this study also does not examine the changes in overall emissions during lockdown compared to business-as-usual; rather, we investigate the relationship between an area's historical emissions and their estimated changes in $PM_{2.5}$ during lockdown. Future work will include investigation of changes in emissions due to lockdowns and the downstream effects on air pollution.

Table 2
Estimates of changes in respiratory and cardiovascular disease hospitalizations owed to lockdown-attributable $PM_{2.5}$ changes for populations age 65+ stratified by US census region, both over the lockdown period ("LD") and in the hypothetical scenario that the $PM_{2.5}$ changes persisted for one year.

Region	Respiratory (LD)	CVD (LD)	Respiratory (Yearly)	CVD (Yearly)
Northeast	35	64	256	469
South	57	105	416	764
Midwest	83	153	609	1117
West	-14	-26	-104	-191
US Total	161	296	1177	2160

Our study has found that the impacts of the 2020 COVID-19 lockdowns on $PM_{2.5}$ levels vary dramatically across the US, with strong regional trends. In the Midwestern and Southern regions, we unexpectedly observe consistent increases in $PM_{2.5}$ compared to expected levels absent the lockdowns, while some areas in the Southwest experienced substantial decreases. One possible reason for this result is that $PM_{2.5}$ in the US is mostly attributed to industrial processes, electricity generation, and dust (Chen et al., 2020), which may have been minimally affected by the COVID-19 lockdowns. This is consistent with the results of several other studies in the US (Archer et al., 2020; Bekbulat et al., 2021; Berman and Ebisu, 2020; Chen et al., 2020) which find either no change or increases in $PM_{2.5}$ over the lockdown period. The reasons behind these trends are undoubtedly intricate given the complex nature of $PM_{2.5}$ formation and a full investigation of these reasons is beyond the scope of this paper.

The results of this important quasi-experiment provide evidence that policies to limit individual-level emissions-generating behaviors like mobility may not, alone, reduce total $PM_{2.5}$ levels, particularly in certain regions and when accompanied by other social and economic changes. Reduction of emissions from stationary sources may be necessary to meaningfully and uniformly reduce $PM_{2.5}$ and improve human health.

Author contributions: KLC led all data preparation, conducted all statistical analyses, and prepared a first draft of the manuscript. LRFH provided expertise in air pollution and atmospheric chemistry and assisted with manuscript preparation. RCN assisted with idea generation and study design, aided in data acquisition and preparation, provided statistical input, and assisted with manuscript preparation.

Data and materials availability: Requests for materials should be addressed to Rachel Nethery at rnethery@hsph.harvard.edu.

Declaration of Competing Interest

Authors declare that they have no competing interests.

Acknowledgements

Funding: This work was supported by the National Institutes of Health [grant numbers T32ES007142, 1K01ES032458-01, R01AG060232].

Supplementary material

Supplementary material associated with this article can be found, in the online version, at 10.1016/j.envadv.2021.100122.

References

Abadie, A., Diamond, A., Hainmueller, J., 2010. Synthetic control methods for comparative case studies: estimating the effect of California's tobacco control program. J. Am. Stat. Assoc. 105 (490), 493–505.
Archer, C.L., Cervone, G., Golbazi, M., Fahel, N.A., Hultquist, C., 2020. Changes in air quality and human mobility in the USA during the COVID-19 pandemic. Bull. Atmos. Sci. Technol. 1 (3–4), 491–514. https://doi.org/10.1007/s42865-020-00019-0.

Athey, S., Bayati, M., Doudchenko, N., Imbens, G., Khosravi, K., 2020. Matrix completion methods for causal panel data models. 1710.10251.

Badr, H.S., Du, H., Marshall, M., Dong, E., Squire, M.M., Gardner, L.M., 2020. Association between mobility patterns and COVID-19 transmission in the USA: a mathematical modelling study. Lancet Infect. Dis. https://doi.org/10.1016/s1473-3099(20)30553-3.

Barré, J., Petetin, H., Colette, A., Guevara, M., Peuch, V.-H., Rouil, L., Engelen, R., Inness, A., Flemming, J., García-Pando, C.P., Bowdalo, D., Meleux, F., Geels, C., Christensen, J.H., Gauss, M., Benedictow, A., Tsyro, S., Friese, E., Struzewska, J., Kaminski, J.W., Douros, J., Timmermans, R., Robertson, L., Adani, M., Jorba, O., Joly, M., Kouznetsov, R., 2021. Estimating lockdown-induced european NO2 changes using satellite and surface observations and air quality models. Atmos. Chem. Phys. 21 (9), 7373–7394. https://doi.org/10.5194/acp-21-7373-2021.

Bekbulat, B., Apte, J.S., Millet, D.B., Robinson, A.L., Wells, K.C., Presto, A.A., Marshall, J. D., 2021. Changes in criteria air pollution levels in the US before, during, and after covid-19 stay-at-home orders: evidence from regulatory monitors. Sci. Total Environ. 769, 144693. https://doi.org/10.1016/j.scitotenv.2020.144693.

Bell, M.L., 2012. Assessment of the health impacts of particulate matter characteristics. Res Rep Health Eff Inst (161), 5–38.

Berman, J.D., Ebisu, K., 2020. Changes in U.S. air pollution during the COVID-19 pandemic. Sci. Total Environ. 739, 139864. https://doi.org/10.1016/j.scitotenv.2020.139864.

Chen, L.-W.A., Chien, L.-C., Li, Y., Lin, G., 2020. Nonuniform impacts of COVID-19 lockdown on air quality over the United States. Sci. Total Environ. 745, 141105.

Clancy, L., Goodman, P., Sinclair, H., Dockery, D.W., 2002. Effect of air-pollution control on death rates in Dublin, Ireland: an intervention study. Lancet 360 (9341), 1210–1214. https://doi.org/10.1016/s0140-6736(02)11281-5.

Dominici, F., Peng, R.D., Bell, M.L., Pham, L., McDermott, A., Zeger, S.L., Samet, J.M., 2006. Fine particulate air pollution and hospital admission for cardiovascular and respiratory diseases. JAMA 295 (10), 1127. https://doi.org/10.1001/jama.295.10.1127.

Friedman, M.S., 2001. Impact of changes in transportation and commuting behaviors during the 1996 Summer Olympic Games in Atlanta on air quality and childhood asthma. JAMA 285 (7), 897. https://doi.org/10.1001/jama.285.7.897.

Gkatzelis, G.I., Gilman, J.B., Brown, S.S., Eskes, H., Gomes, A.R., Lange, A.C., McDonald, B.C., Peischl, J., Petzold, A., Thompson, C.R., Kiendler-Scharr, A., 2021. The global impacts of COVID-19 lockdowns on urban air pollution. Elem. Sci. Anth. 9 (1) https://doi.org/10.1525/elementa.2021.00176.

Gorelick, N., Hancher, M., Dixon, M., Ilyushchenko, S., Thau, D., Moore, R., 2017. Google earth engine: planetary-scale geospatial analysis for everyone. Remote Sens. Environ. https://doi.org/10.1016/j.rse.2017.06.031.

He, G., Pan, Y., Tanaka, T., 2020. The short-term impacts of COVID-19 lockdown on urban air pollution in China. Nat. Sustain. 3 (12), 1005–1011. https://doi.org/10.1038/s41893-020-0581-y.

Herdağdelen, A., Dow, A., State, B., Mohassel, P., Pompe, A., 2020. Protecting privacy in facebook mobility data during the COVID-19 response. https://research.fb.com/blog/2020/06/protecting-privacy-in-facebook-mobility-data-during-the-covid-19-response/.

Hou, Q., An, X., Wang, Y., Guo, J., 2010. An evaluation of resident exposure to respirable particulate matter and health economic loss in Beijing during Beijing 2008 Olympic Games. Sci. Total Environ. 408 (19), 4026–4032. https://doi.org/10.1016/j.scitotenv.2009.12.030.

Ingram, D.D., Franco, S.J., 2012. NCHS urban-rural classification scheme for counties. Vital Health Stat 2 (154), 1–65.

Jacobsen, G.D., Jacobsen, K.H., 2020. Statewide COVID-19 stay-at-home orders and population mobility in the United States. World Med. Health Policy. https://doi.org/10.1002/wmh3.350.

Kloog, I., Coull, B.A., Zanobetti, A., Koutrakis, P., Schwartz, J.D., 2012. Acute and chronic effects of particles on hospital admissions in New-England. PLoS ONE 7 (4), e34664. https://doi.org/10.1371/journal.pone.0034664.

Lasry, A., Kidder, D., Hast, M., Poovey, J., Sunshine, G., Winglee, K., Zviedrite, N., Ahmed, F., Ethier, K.A., Clodfelter, C., Howard-Williams, M., Hulkower, R., Jeong, G., Landsman, L., McCord, R., Moreland, A., Shelburne, J., Billioux, A., Hand, J., Kanter, J., Smith, A., Sokol, T., Duchin, J.S., Fagalde, M.S., Pogosjans, S., Brown, R., Huang, S., Moss, N., Pan, E., Shemsu, M., Yette, E., Bock, C., Curtis-Robles, R., Lockett, C., Morrow, S., Sallenave, C., Santora, L., Willis, M., 2020. Timing of community mitigation and changes in reported COVID-19 and community mobility– Four U.S. metropolitan areas. MMWR Morb. Mortal. Wkly. Rep. 69 (15), 451–457. https://doi.org/10.15585/mmwr.mm6915e2.February 26–April 1, 2020

Li, Y., Wang, W., Kan, H., Xu, X., Chen, B., 2010. Air quality and outpatient visits for asthma in adults during the 2008 Summer Olympic Games in Beijing. Sci. Total Environ. 408 (5), 1226–1227. https://doi.org/10.1016/j.scitotenv.2009.11.035.

Liu, F., Wang, M., Zheng, M., 2021. Effects of COVID-19 lockdown on global air quality and health. Sci. Total Environ. 755, 142533. https://doi.org/10.1016/j.scitotenv.2020.142533.

Menut, L., Bessagnet, B., Siour, G., Mailler, S., Pennel, R., Cholakian, A., 2020. Impact of lockdown measures to combat COVID-19 on air quality over Western Europe. Sci. Total Environ. 741, 140426. https://doi.org/10.1016/j.scitotenv.2020.140426.

Murray, C.J.L., Aravkin, A.Y., Zheng, P., Abbafati, C., Abbas, K.M., Abbasi-Kangevari, M., Abd-Allah, F., Abdelalim, A., Abdollahi, M., Abdollahpour, I., Abegaz, K.H., Abolhassani, H., Aboyans, V., 2020. Global burden of 87 risk factors in 204 countries and territories, 1990–2019: a systematic analysis for the global burden of disease study 2019. Lancet 396 (10258), 1223–1249. https://doi.org/10.1016/s0140-6736(20)30752-2.

Pope, C.A., 2000. Epidemiology of fine particulate air pollution and human health: biologic mechanisms and who's at risk? Environ. Health Perspect. 108 (suppl 4), 713–723. https://doi.org/10.1289/ehp.108-1637679.

Putaud, J.-P., Pozzoli, L., Pisoni, E., Santos, S.M.D., Lagler, F., Lanzani, G., Santo, U.D., Colette, A., 2021. Impacts of the COVID-19 lockdown on air pollution at regional and urban background sites in Northern Italy. Atmos. Chem. Phys. 21 (10), 7597–7609. https://doi.org/10.5194/acp-21-7597-2021.

Raifman, J., Nocka, K., Jones, D., Bor, J., Lipson, S., Jay, J., Chan, P., 2020. COVID-19 US state policy database. Available at: www.tinyurl.com/statepolicies.

Shakoor, A., Chen, X., Farooq, T.H., Shahzad, U., Ashraf, F., Rehman, A., e Sahar, N., Yan, W., 2020. Fluctuations in environmental pollutants and air quality during the lockdown in the USA and China: two sides of COVID-19 pandemic. Air Qual. Atmos. Health 1–8.

U.S. Census Bureau, 2019. 2014–2018 American Community Survey 5-Year Estimates. Prepared by Social Explorer.

U.S. Environmental Protection Agency, 2014. National emissions inventory. https://www.epa.gov/air-emissions-inventories/2014-national-emissions-inventory-nei-data.

U.S. Environmental Protection Agency, 2017. National emissions Inventory. https://www.epa.gov/air-emissions-inventories/2017-national-emissions-inventory-nei-data.

U.S. Environmental Protection Agency, 2020a. Air quality system data mart. http://www.epa.gov/ttn/airs/aqsdatamart.

U.S. Environmental Protection Agency, 2020b. Environmental benefits mapping and analysis program - community edition.

U.S. Environmental Protection Agency, 2020c. Our Nation's Air 2020. https://gispub.epa.gov/air/trendsreport/2020.

Xing, Y.-F., Xu, Y.-H., Shi, M.-H., Lian, Y.-X., 2016. The impact of PM2.5 on the human respiratory system. J. Thorac. Dis. 8 (1) https://doi.org/10.3978/j.issn.2072-1439.2016.01.19.http://jtd.amegroups.com/article/view/6353

Xu, Y., 2017. Generalized synthetic control method: causal inference with interactive fixed effects models. Polit. Anal. 25 (1), 57–76. https://doi.org/10.1017/pan.2016.2.